JOURNAL OF APPLIED ELECTROCHEMISTRY 16 (1986) 836–850

*Selectivity analysis in electrochemical reactors. I. Experimental study of an electro-organic reaction coupled with parasitic homogeneous chemical reactions**

L. WEISE, G. VALENTIN, A. STORCK

Laboratoire des Sciences du Génie Chimique, CNRS–ENSIC, 1 rue Grandville, 54042 Nancy Cedex, France

R. MAUGE, A. COHEN

Société ORIL, 76210 Bolbec, France

Received 11 March 1986; revised 14 July 1986

The electrochemical reduction of *N*-nitroso-2-methylindoline to *N*-amino-2-methylindoline is studied experimentally using a batch stirred-tank electrochemical reactor. The influence of important parameters such as temperature, specific electrode area, hydrodynamics of the electrolyte, and initial reactant concentration are examined to quantify their effect on the overall process selectivity. It is shown that the product yield is very sensitive to these parameters due to the complex chemical reaction sequence coupled with the desired heterogeneous electrochemical reaction.

Nomenclature

A_e	electrode area (m^2)
a_e	specific electrode area (m^{-1})
C_A, C_B, C_C	molar concentrations of species A, B, C ($mol\,m^{-3}$)
D_A	molecular diffusion coefficient of A ($m^2\,s^{-1}$)
E	electrode potential (V)
F	Faraday's constant
I	current intensity (A)
i	current density ($A\,m^{-2}$)
k_c	chemical rate constant of scheme II ($s^{-1}\,mol^{-1}\,m^3$)
k_{ci}	chemical rate constants involved in scheme I (see Table 2)
k_d	mass transfer coefficient ($m\,s^{-1}$)
r_i	chemical reaction rate ($mol\,m^{-3}\,s^{-1}$)
N	impeller rotation speed (r.p.s.)
S	product selectivity = $X_B/(1 - X_A)$
t	time (s)
V	volume of catholyte (m^3)
X_A, X_B, X_C	molar fractions, i.e. C_{AS}/C_{A0}; C_{BS}/C_{A0}; C_{CS}/C_{A0}
X'_B	molar fraction = C_{BS}/C_{B0}
X'_C	molar fraction = $C_{CS}/(C_{A0} + C_{B0} + C_{C0})$
ν_e	number of electrons involved in the reduction
ν	kinematic viscosity of electrolyte ($m^2\,s^{-1}$)

Subscripts

0	initial (time = 0)
L	limiting
S	in the bulk of the electrolyte

* This paper was presented at the meeting on 'Electroorganic Process Engineering' held in Perpignan, France, 19–20 September 1985.

0021–891X/86 $03.00 + .12

1. Introduction

In recent years considerable efforts have been made to develop electrochemical processes for the industrial production of high value organic compounds. In many such systems electrochemical reactions are coupled at the electrode–electrolyte interface with homogeneous chemical reactions which occur in the bulk solution and close to the electrodes.

The design of electrochemical reactors to produce a desired product depends not only on the electrochemistry at the working electrode but also on the operating conditions of the cell, characterized by:

(i) the type of electrolytic cell used (batch, continuous-stirred tank or piston flow reactor, etc.
(ii) the geometric parameters (specific electrode area etc.)
(iii) hydrodynamic factors
(iv) the electrochemical mode of operation (potentiostatic or galvanostatic).

The sensitivity of the product yield to these parameters and the effect of mass transport, fluid mixing, current distribution, space time, etc. are important factors in considering the optimum selectivity control of a process. This general problem has recently been investigated by several authors. For the hydrodimerization of acrylonitrile and the methoxylation of furan, Tomov and Jansson [1] have shown that cells with different mixing conditions give different performances (distribution of products) for the same reaction under the same nominal conditions. Sakellaropoulos and Francis [2] have proposed a general methodology for predicting the selectivity of two model reactors (channel plug flow or complete mixing) for parallel electrochemical reactions. Amatore and Saveant [3–6] have discussed the relationships between the distribution of products and characteristic rates or rate ratios and the magnitude of the operational parameters for different reaction schemes encountered in a large variety of electrochemical processes. However, in this latter study the analysis was restriced to chemical reactions with high values of the rate constant and occurring therefore only in a reaction layer inside a diffusion boundary layer.

This paper (Part I) presents an experimental analysis of the selectivity in an electro-organic process, where the main desired electrochemical reduction is coupled with unwanted homogeneous chemical reactions between the reactant A and the required product B. (A theoretical analysis of this selectivity is presented in Part II [7].) The specific example investigated here has the following simplified mechanism. (For a complete discussion, see paragraph 3.1.)

$$\begin{aligned} A + 4e &\longrightarrow B && \text{required electrochemical reaction} \\ A + B &\longrightarrow 2C && \text{homogeneous chemical side reaction} \end{aligned} \qquad (1)$$

with

A = 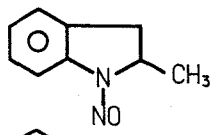 *N*-nitroso-2-methylindoline

B = 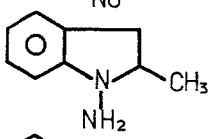 *N*-amino-2-methylindoline

C = 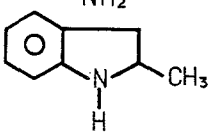 2-methylindoline

Product B is a high-value substrate used to prepare a pharmaceutical compound, and its synthesis therefore requires a high selectivity for the electrochemical route to be competitive with the chemical

route of hydrogenation using a mixed aluminium hydride. Mechanism 1 was first investigated in an acidic media by Jacob and co-workers [8, 9], who showed that preparative electrolysis of A yielded a mixture of B and C, emphasizing the selectivity problem involved in this process.

Part I of this study presents an experimental analysis of a batch stirred-tank electrochemical reactor involving the influence of important parameters such as mixing conditions, interfacial electrode area and reactant concentration on the product yield, and a discussion of the complete mechanism involved. Part II [7] deals with a theoretical approach to selectivity based on classical models, concepts and approximations used in heterogeneous multiphase contactors.

2. Experimental details

2.1. *Apparatus*

A schematic view of the batch stirred-tank electrochemical reactor used in the experiments is shown

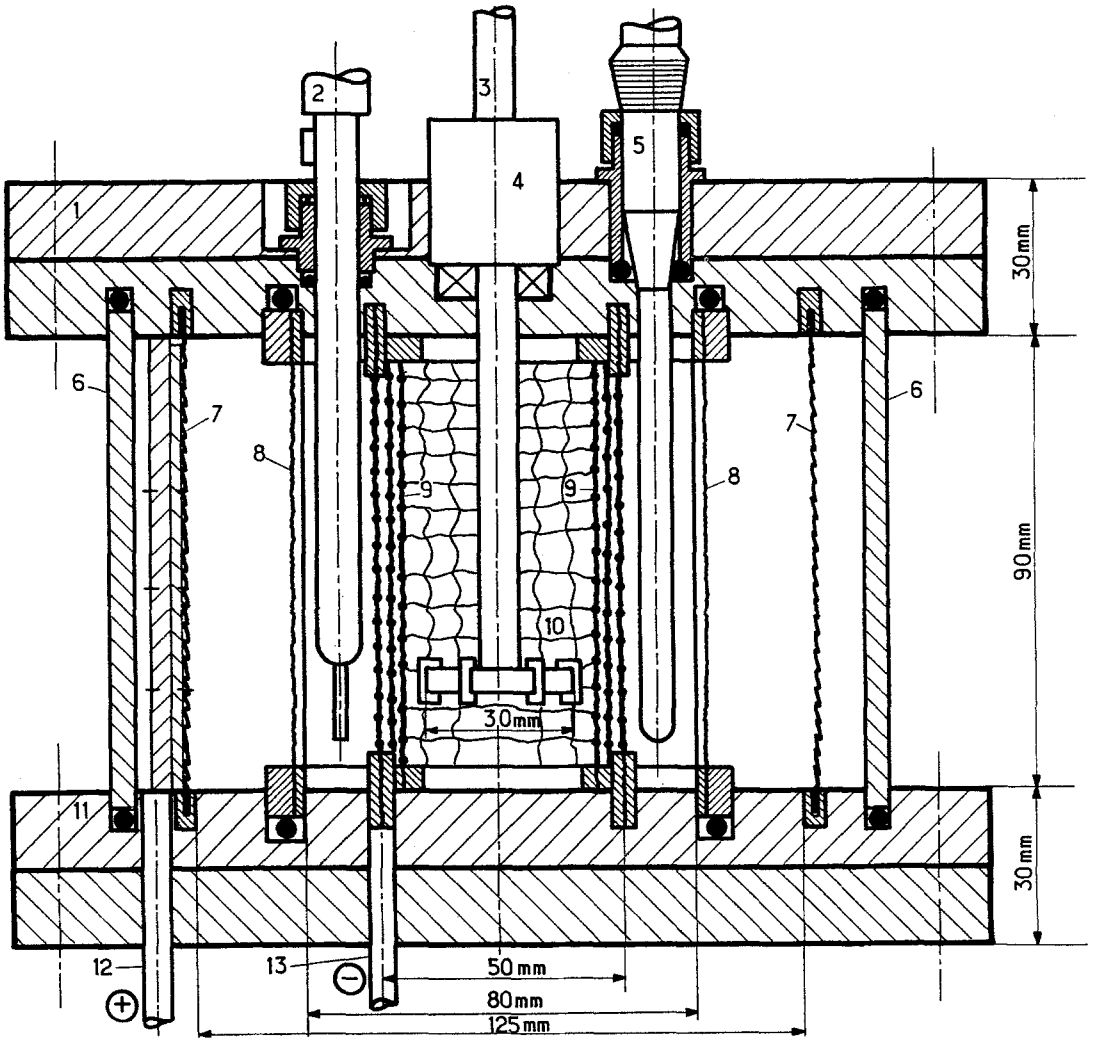

Fig. 1. Schematic view of the batch stirred-tank electrochemical reactor. 1, lid, CPV translucid; 2, reference electrode; 3, axis of stirrer; 4, ball bearing; 5, glass electrode; 6, external shell; 7, anode; 8, cationic exchange membrane; 9, cathode grids; 10, stirrer; 11, bottom, CPV translucid; 12, anodic current feeder; 13, cathodic current feeder.

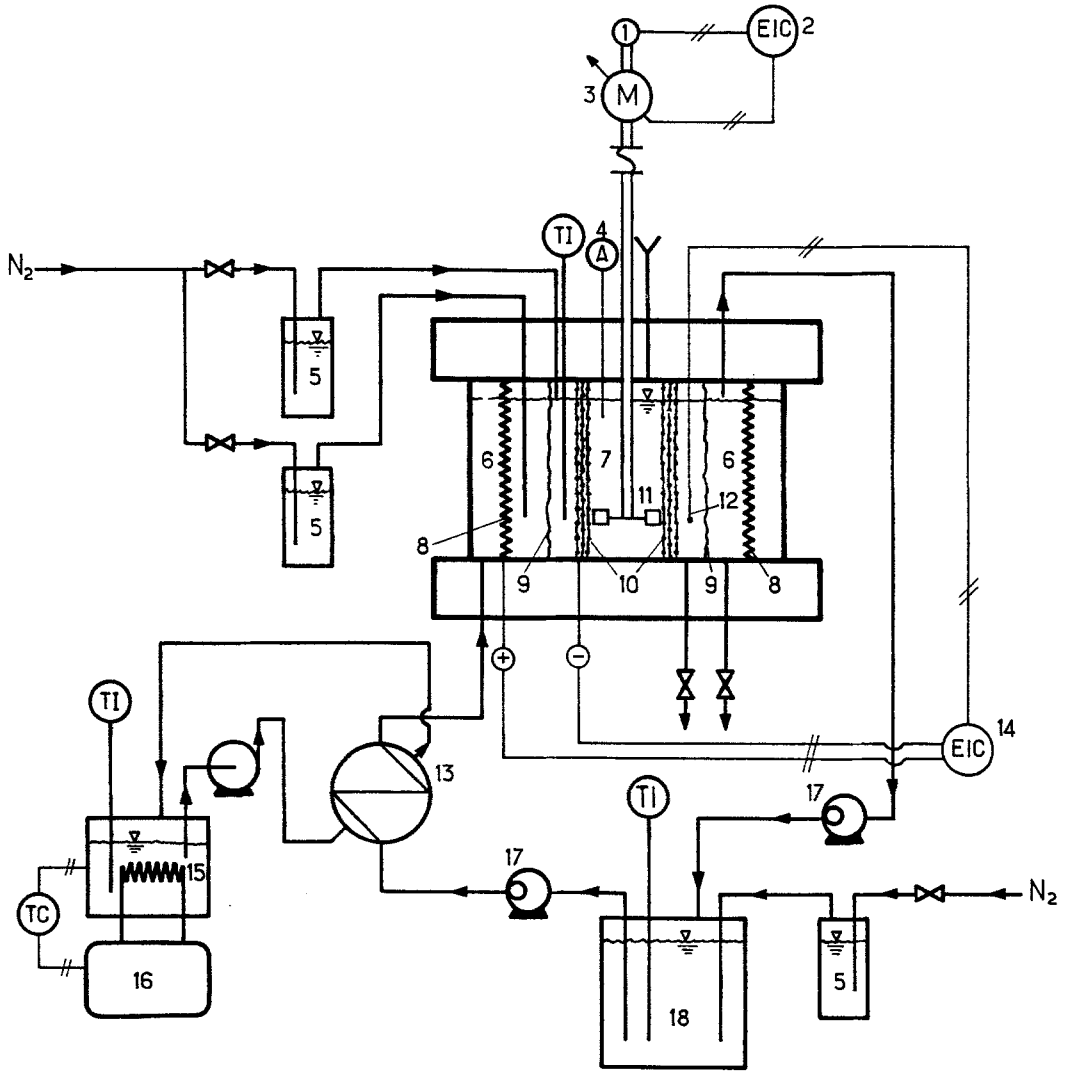

Fig. 2. Schematic view of the installation. 1, tachometer; 2, speed variator, speed control and speed indication; 3, motor; 4, sampling for analysis; 5, wash-flask; 6, anodic compartment; 7, cathodic compartment; 8, anode; 9, membrane; 10, cathode grids; 11, stirrer; 12, reference electrode; 13, cooler; 14, potentiostat, current recorder and potential indication; 15, thermostatic bath; 16, cooling unit; 17, peristaltic pump; 18, anolyte storage tank.

in Figs 1 and 2. It consists of a series of co-axial cylinders (in an outward direction from the reactor axis, these are: cathode, membrane, anode and reactor wall) with a six-bladed turbine agitator located centrally. The working electrode (cathode) is composed of one or several expanded metal grids of copper amalgam prepared electrochemically. The anode, where oxygen evolution occurs, is a cylinder of platinized titanium located against the cylindrical wall of the reactor. A cation exchange membrane (IONAC 3470) fixed on a cylindrical mesh CPV support separates the two cell compartments which have volumes of 0.48 litres for the cathodic side and 1.00 litres for the anodic side. As shown in Fig. 2, a recirculation of the anolyte (a mixture of equal parts by volume of 5 N H_2SO_4 and pure ethanol) through an outside chamber allows the separation of oxygen from the anolyte as well as temperature control. The rotation speed of the impeller was varied between 250 and 1000 r.p.m.

Table 1. Influence of temperature and reactant concentration on the molecular diffusion coefficient, D_A ($m^2 s^{-1}$)

T (K)	C_{AS} ($mol\,m^{-3}$)					
	1	*4*	*12*	*20*	*40*	*50*
283	1.18×10^{-10}	1.13×10^{-10}	1.10×10^{-10}	1.10×10^{-10}	1.10×10^{-10}	1.10×10^{-10}
298	2.74×10^{-10}	2.65×10^{-10}	2.42×10^{-10}	2.28×10^{-10}	2.00×10^{-10}	1.95×10^{-10}

2.2. *Analysis of the components and physicochemical properties of the catholyte*

Two different methods were used for the titrations of A, B and C in the catholyte, which is a mixture of 5 N H_2SO_4 and EtOH (proportion 1:1 by volume), and which contained only the reactant A at the beginning of the electrolysis. Impulse differential mercury drop polarography (Metrohm Polarecord E506) was used for components A and B; HPTLC (Shimadzu, Scanner CS 920, using precoated plates of Silica Gel 60) was used for B and C. The detailed conditions of the analysis are described in [10].

The physicochemical properties of the catholytes, i.e. kinematic viscosity (ν) and diffusion coefficient (D_A) of the reactant in the electrolyte, were determined by capillary viscometry and Levich's method on an amalgamated copper rotating disc (5.42 mm), respectively. The influences of the temperature T (K) and bulk concentration, C_{AS}, were determined leading to the following relationship for ν [10]:

$$\nu = 1.309 \exp(-4.54 \times 10^{-3} T) + 1.0 \times 10^{-6} (m^2 s^{-1})$$

valid for $278 < T < 313$ K ($\nu = 3.18 \times 10^{-6} m^2 s^{-1}$ for $T = 293$ K). No influence of C_{AS} and C_{BS} on ν was observed in the range of concentrations considered in this study. Table 1 presents the variations of D_A with the bulk concentration C_{AS} (for $C_{BS} = 0$), for two different temperatures (283 and 298 K). The temperature, which has an important effect on the rate constant of the homogeneous reaction (see Mechanism 1), also significantly modifies the values of D_A (and consequently the electrochemical reaction rate) whereas, for $C_{AS} > 30\,mol\,m^{-3}$, no influence of C_{AS} is observed.

3. Results

3.1. *Chemical mechanisms involved in an electrolyte containing N-nitroso-2-methyl-indoline and N-amino-2-methyl-indoline*

Jacob and co-workers [8, 9] have shown that for particular experimental conditions, the reactant A and the product B are involved in several chemical reactions occurring simultaneously under different reaction rates. In order to generalize the overall scheme proposed in [8] and to derive values for the chemical rate constants of the mechanisms involved, several experiments have been performed in a batch chemical stirred-tank reactor maintained at a constant temperature. The solvent used (5 N H_2SO_4–EtOH, 1:1 by volume) was the same as for the electrochemical preparative electrolysis (paragraph 3.2) and was protected against light and oxygen.

N-nitroso-2-methylindoline (A) is relatively stable in aprotic solutions but not in the aqueous acidic media used in this work. In order to describe the degradation of A alone in the specific electrolyte mentioned above, the following reaction schemes are proposed:

$$A + H^+ \rightleftharpoons AH^+ \quad (a)$$

$$AH^+ \rightleftharpoons C + NO^+ \quad (b)$$

$$NO^+ + EtOH \longrightarrow EtONO + H^+ \quad (c)$$

Equilibrium (a) should be rapidly achieved and deplaced to the right in strongly acidic solutions. Mechanism (c), involving the reaction of the nitrosylcation with ethanol, is probably very slow and perhaps even controlled by the rate of evaporation of EtONO.

The product B (*N*-amino-2-methylindoline) is more or less stable in aqueous acid solution when no reactant A and NO^+ are present. Otherwise, as proposed in [8], the following fast reaction has to be considered:

$$B + NO^+ \longrightarrow C + N_2O + H^+ \qquad (d)$$

Finally it should be mentioned that in strongly acidic electrolytes the protonation of B through

$$B + H^+ \rightleftharpoons BH^+ \qquad (e)$$

may also be important.

These five reactions constitute the basis of the first scheme proposed.

		Kinetic constant
Scheme I	$A + H^+ \rightleftharpoons C + NO^+$	k_{C1}, k_{C-1}
	$NO^+ + EtOH \longrightarrow EtONO + H^+$	k_{C2} (slow reaction)
	$B + NO^+ \longrightarrow C + N_2O + H^+$	k_{C3}
	$B + H^+ \rightleftharpoons BH^+$	k_{C4}, k_{C-4}

In this scheme, equilibriums (a) and (b) have been summed into a single equation.

The rate constant, k_{C2}, can be easily determined experimentally by following the rate of degradation of reactant A alone in the batch reactor; indeed by considering that reaction (c) is very slow, the overall degradation of A may be reduced to:

$$A + EtOH \xrightarrow[k_{C2}]{H^+} C + EtONO \qquad (f)$$

The values of the pseudo first-order rate constant $k'_{C2} = k_{C2}[EtOH]$ obtained through this procedure are reported in Table 2 for two different temperatures. In the more general case, where A and B are simultaneously present in a solution, the validity of scheme I has been verified by comparing the experimental results of the time variations of C_{AS}, C_{BS} and C_{CS} (reported in the form of C_{AS}/C_{A0}, C_{BS}/C_{B0} and $C_{CS}/(C_{A0} + C_{B0} + C_{C0})$ with time t) with the calculated results using the general scheme I.

Table 2. Values of the chemical rate constants for schemes I and II

Rate constant	*T (K)*		*Unit*
	283	*298*	
Scheme I			
$k'_{C1} = k_{C1}\lvert H^+\rvert$	5.53×10^{-4}	9.34×10^{-3}	s^{-1}
k_{C-1}	1.01×10^{-2}	3.35×10^{-3}	$s^{-1}\,mol^{-1}\,m^3$
k'_{C2}	1.39×10^{-6}	7.87×10^{-6}	s^{-1}
k_{C3}	5.51	2.66×10^{-1}	$s^{-1}\,mol^{-1}\,m^3$
$k'_{C4} = k_{C4}\lvert H^+\rvert$	8.51×10^{-1}	4.56×10^{-1}	s^{-1}
k_{C-4}	2.85×10^{-3}	8.07×10^{-4}	s^{-1}
Scheme II			
k_C	1.08×10^{-5}	1.70×10^{-5}	$s^{-1}\,mol^{-1}\,m^3$

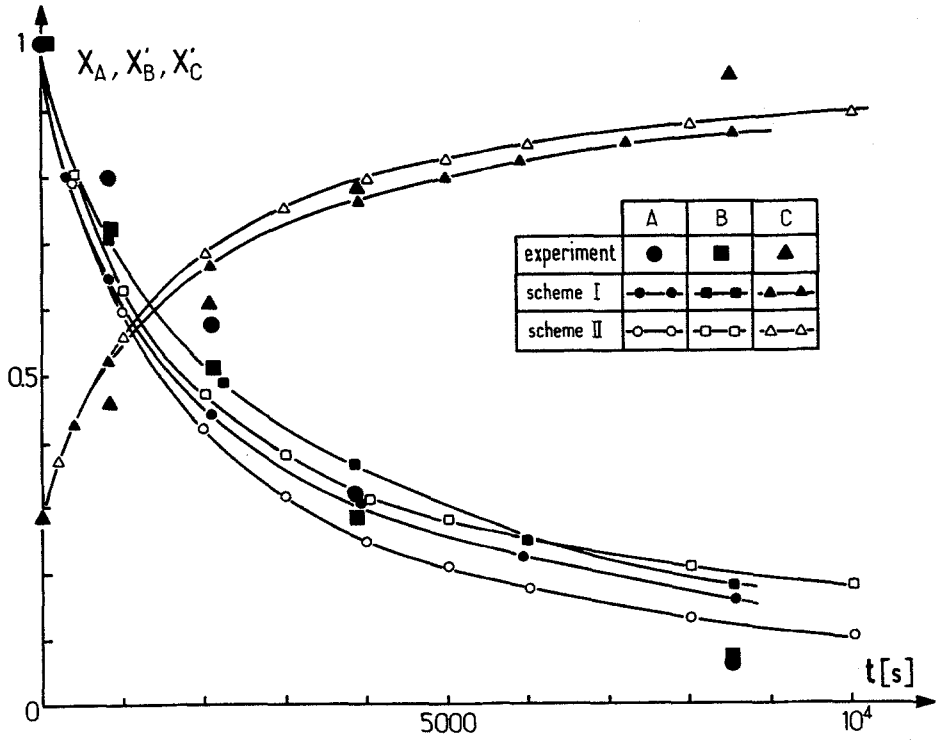

Fig. 3. Time variations of the concentrations for the chemical reactions between reactant A and product B. Experimental and calculated results. $T = 298\,K$; $V = 4.8 \times 10^{-4}\,m^3$; $C_{A0} = 35.05\,mol\,m^{-3}$; $C_{B0} = 38.53\,mol\,m^{-3}$; $C_{C0} = 29.70\,mol\,m^{-3}$.

These calculations were performed by numerical integration (Runge–Kutta method) of the mass balance equations written for each species j:

$$\frac{dC_j}{dt} + \sum_i \nu_{ij} r_i = 0 \tag{2}$$

Figs 3 and 4 present this comparison for two different sets of initial values for C_{A0}, C_{B0}, C_{C0} and show that the agreement is quite satisfactory for the range of concentration ratios covered by this investigation. The values of the five unknown rate constants defining scheme I derived through a suitable best-fit method are reported in Table 2, which confirms the hypothesis that reaction (c) is comparatively slow. It should be mentioned, however, that the complete scheme I leads to long calculations and we have proposed a simplified mechanism which should lead to a great simplification of the overall problem of considering coupling between the chemical and electrochemical reactions (Section 3.2 and Part II of this work).

This simplified mechanism (scheme II) is as follows:

$$A + B \xrightarrow{k_c} 2C + N_2O \qquad \text{(Scheme II)}$$

which is the result of the summation of (a), (b) and (d), neglecting reactions (c) and (e). Its main advantage is the possibility of obtaining analytical expressions for the time variations of the concentrations in a batch experiment, since the mass balance equations are now reduced to:

$$\frac{dC_{AS}}{dt} = \frac{dC_{BS}}{dt} = -k_c C_{AS} C_{BS} \tag{3$_1$}$$

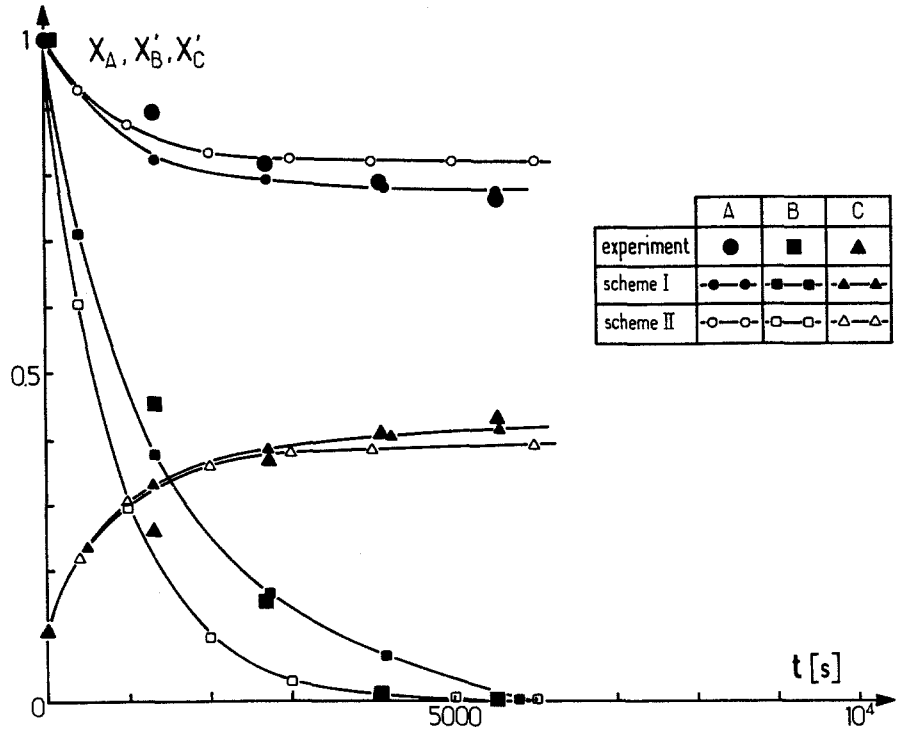

Fig. 4. Time variations of the concentrations for the chemical reactions between A and B. Experimental and calculated results. $T = 298\,\mathrm{K}$; $V = 4.8 \times 10^{-4}\,\mathrm{m}^3$; $C_{A0} = 77.87\,\mathrm{mol\,m^{-3}}$; $C_{B0} = 14.42\,\mathrm{mol\,m^{-3}}$; $C_{C0} = 11.43\,\mathrm{mol\,m^{-3}}$.

and

$$\frac{dC_{CS}}{dt} = 2k_c C_{AS} C_{BS} \tag{3$_2$}$$

with the boundary conditions

$$t = 0, \quad C_{AS} = C_{A0}, \quad C_{BS} = C_{B0}, \quad C_{CS} = C_{C0}$$

Integration of Equations 3_1 and 3_2 leads to the following expressions for $C_{A0} \neq C_{B0}$:

$$X_A = \frac{C_{B0} - C_{A0}}{C_{B0} \exp\left[k_C t(C_{B0} - C_{A0})\right] - C_{A0}} \tag{4$_1$}$$

$$X'_B = \frac{C_{A0} - C_{B0}}{C_{A0} \exp\left[k_C t(C_{A0} - C_{B0})\right] - C_{B0}} \tag{4$_2$}$$

$$X'_C = 1 - \frac{X_A C_{A0} + X'_B C_{B0}}{C_{A0} + C_{B0} + C_{C0}} \tag{4$_3$}$$

and for $C_{A0} = C_{B0}$

$$X_A = X'_B = \frac{1}{k_C C_{A0} t + 1} \tag{4$_4$}$$

$$X'_C = 1 - \frac{2X_A C_{A0}}{2C_{A0} + C_{C0}} \tag{4$_5$}$$

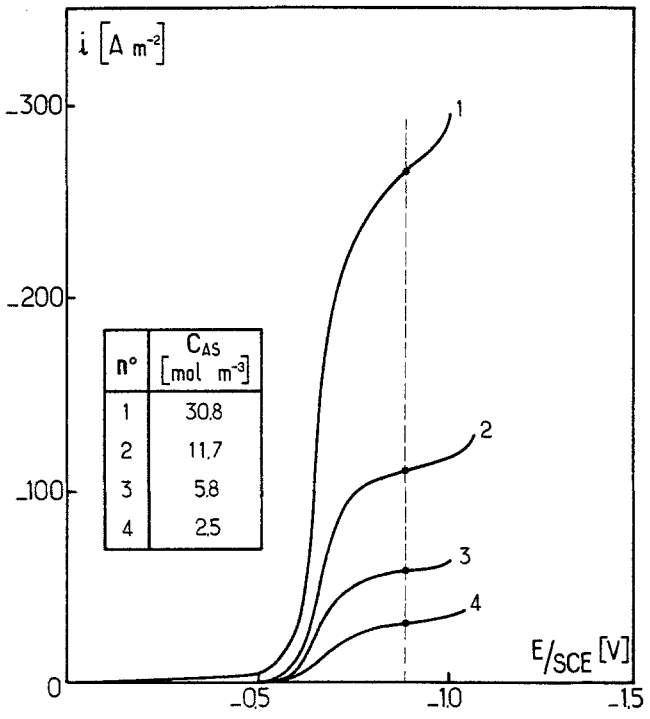

Fig. 5. Examples of current density–electrode potential curves obtained in the stirred-tank electrochemical reactor. $N = 1000$ r.p.m.; $T = 298$ K; $A_e = 5.54 \times 10^{-2}$ m^2.

The rate constant, k_C, is determined by comparing the experimental results with Equations 4_1–4_5. Such a comparison is presented in Figs 3 and 4, which show relatively good agreement with the experimental results and also with those calculated through the more complex scheme I. Consequently, this simplified scheme may correctly represent the overall chemical reactions involved as a first approximation. The values of k_C deduced from a least squares optimization based on several experimental runs with different initial concentrations are reported in Table 2 for two temperatures.

3.2. *Electrochemical macroscopic kinetics (static analysis) and preparative electrolysis of B (dynamic analysis)*

3.2.1. Electrochemical kinetics. For a given impeller rotation speed, N, and different values of C_{AS}, in conditions such that C is small enough for the influence of the chemical reactions to be neglected in the time scale of an experiment (see Part II of this work [7]), Fig. 5 presents typical current density–potential curves obtained inside the stirred electrochemical reactor. A relatively flat

Table 3. Values of the mass transfer coefficient, k_d, under different operating conditions

T (K)	A_e (m^2)	N (r.p.s.)	$k_d \times 10^5$ (ms^{-1})
298	2.05×10^{-2}	8.33	1.75
298	2.05×10^{-2}	16.67	3.11
298	5.54×10^{-2}	4.17	1.07
298	5.54×10^{-2}	8.33	1.61
298	5.54×10^{-2}	16.67	2.23
283	5.54×10^{-2}	16.67	1.77

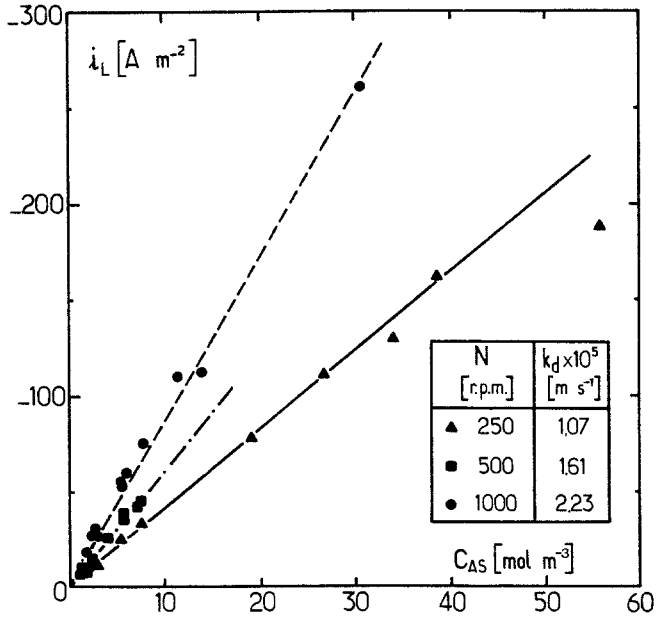

Fig. 6. Experimental plots of the limiting current density i_L versus C_{AS} when $T = 298$ K and $A_e = 5.54 \times 10^{-2}$ m^2.

diffusion plateau is observed, except for higher concentrations where a larger inclination occurs, probably due to current distribution problems. As mentioned by Jacob and co-workers [8], this polarogram characterizes the four-electron cathodic wave of 1-nitroso-2 methylindoline. From Fig. 5 and others not presented here [10], it can be concluded that an electrode potential between -1000 and -800 mV versus SCE should correspond closely to conditions of pure diffusional limitations whatever the values of T, N and C_{AS}. For $T = 298$ K and $A_e = 5.5 \times 10^{-2}$ m^2, Fig. 6 shows that the variations of the limiting current density, i_L, with C_{AS} are effectively linear for a given rotation speed. The slopes of these lines give the values of the mass transfer coefficient, k_d, between the mesh electrode and the catholyte.

Table 3 presents the values of k_d obtained through this procedure for different hydrodynamic and geometric conditions; it should be mentioned that the modification of the area, A_e, of the working electrode (from $A_e = 2.05 \times 10^{-2}$ m^2 with one mesh electrode to $A_e = 5.5 \times 10^{-2}$ m^2 obtained with three smaller electrodes) leads to different values of k_d for a given value of N. This may be explained through the perturbation generated in the hydrodynamic field by additional mesh cathodes.

3.2.2. Performance of preparative electrolyses. Preparative electrolyses were carried out potentiostatically by fixing the cathode potential at a value between -1000 and -800 mV versus SCE in order to operate under limiting current conditions which correspond to the maximum value of the electrochemical reaction rate. The influences of the following parameters were considered: temperature, impeller rotation speed, specific electrode area and initial concentration (C_{A0}) of reactant A. The time variations of the bulk concentations C_{AS}, C_{BS}, C_{CS} (or preferably $X_A = C_{AS}/C_{A0}$, $X_B = C_{BS}/C_{A0}$ and $X_C = C_{CS}/C_{A0}$) and of the current intensity, I, as well as the selectivity, S, defined by

$$S = \frac{C_{BS}}{C_{A0} - C_{AS}} = \frac{X_B}{1 - X_A} \tag{5}$$

were measured for each experiment. Figs 7–12 present chosen examples of typical experimental results, which lead to very different process selectivities under different operating conditions.

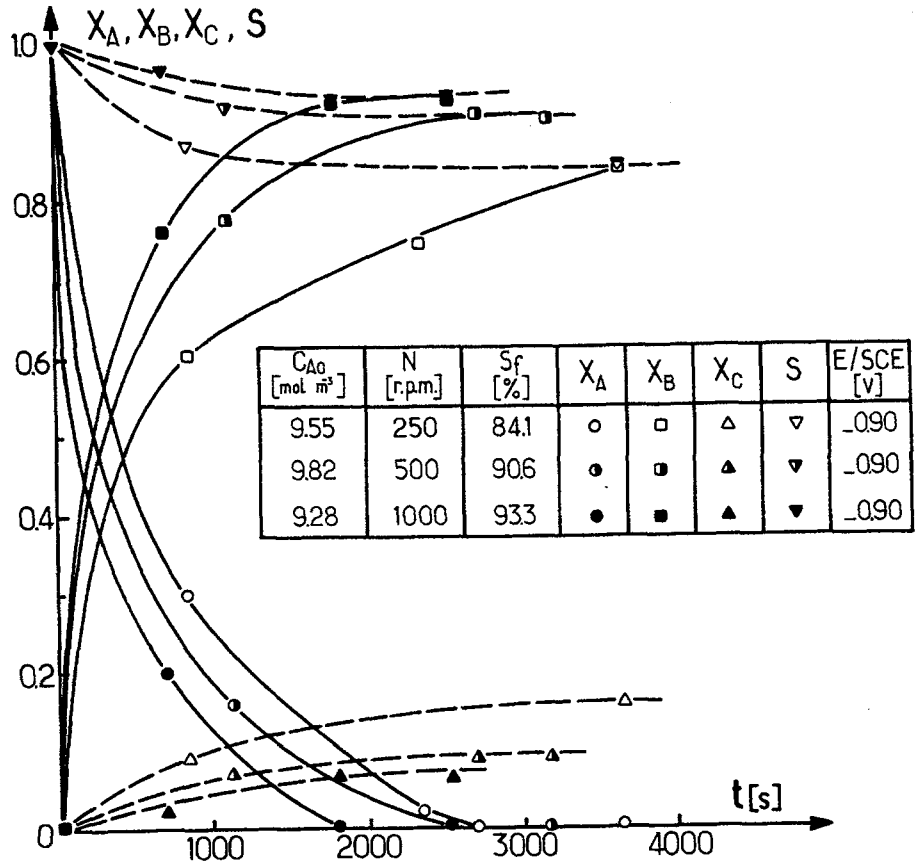

C_{A0} [mol m^{-3}]	N [r.p.m.]	Sf [%]	X_A	X_B	X_C	S	E/SCE [V]
9.55	250	84.1	o	□	△	▽	-0.90
9.82	500	90.6	◐	◨	▲	▼	-0.90
9.28	1000	93.3	●	■	▲	▼	-0.90

Fig. 7. Experimental time variations of the molar fractions X_A, X_B, X_C and the selectivity, S, when $T = 298$ K and $a_e = 115.3\,m^{-1}$. Influence of the fluid mixing.

For all conditions (see Figs 7 and 8) the ratio X_A and the selectivity, S, decrease with time, whereas X_B (desired product) and X_C (unwanted product) increase to limiting values obtained when the conversion factor $(1 - X_A)$ of the reactant is 100% ($C_{AS} = 0$).

3.2.2.1. Influence of the stirrer rotation speed (Fig. 7). For a given temperature and a small initial concentration ($C_{AO} \simeq 10\,mol\,m^{-3}$) the rotation speed has a strong influence on S, which increases when N is higher (see Fig. 7). As an example, for $T = 298$ K, the final selectivity (obtained when $C_{AS} = 0$) is 84.1% for $N = 250$ r.p.m. and 93.3% for $N = 1000$ r.p.m. This effect is attributed to the decrease of the boundary layer thickness, δ, when N increases.

3.2.2.2. Influence of the temperature (Fig. 9). For a given impeller rotation speed, the decrease of the temperature (from 298 to 283 K) leads to an increase in the selectivity. This effect is shown in Fig. 9, which gives variations of S with the electrical charge, Q, passed through the cell. For $N = 1000$ r.p.m., S varies from 93.3% (at a temperature of 298 K) to 95.7% (for $T = 283$ K). This may be explained by two simultaneous effects of a lower temperature: (i) a smaller mass transfer coefficient k_d (when $N = 1000$ r.p.m., $k_d = 2.23 \times 10^{-5}\,m\,s^{-1}$ at $T = 298$ K and $k_d = 1.77 \times 10^{-5}\,m\,s^{-1}$ at $T = 283$ K) and consequently a smaller electrochemical reaction rate; (ii) a decrease in the chemical rate constant (corresponding values of k_c are 1.70×10^{-5} and $1.08 \times 10^{-5}\,s^{-1}\,mol^{-1}\,m^3$). However, in the range of temperature considered in this work the second effect is more pronounced with an overall favourable influence on the selectivity.

3.2.2.3. Influence of the initial concentration and specific electrode area. The influences of C_{A0} and a_e are shown in Figs 8 and 10, which indicate that an increase of C_{A0} and/or a decrease of a_e are very

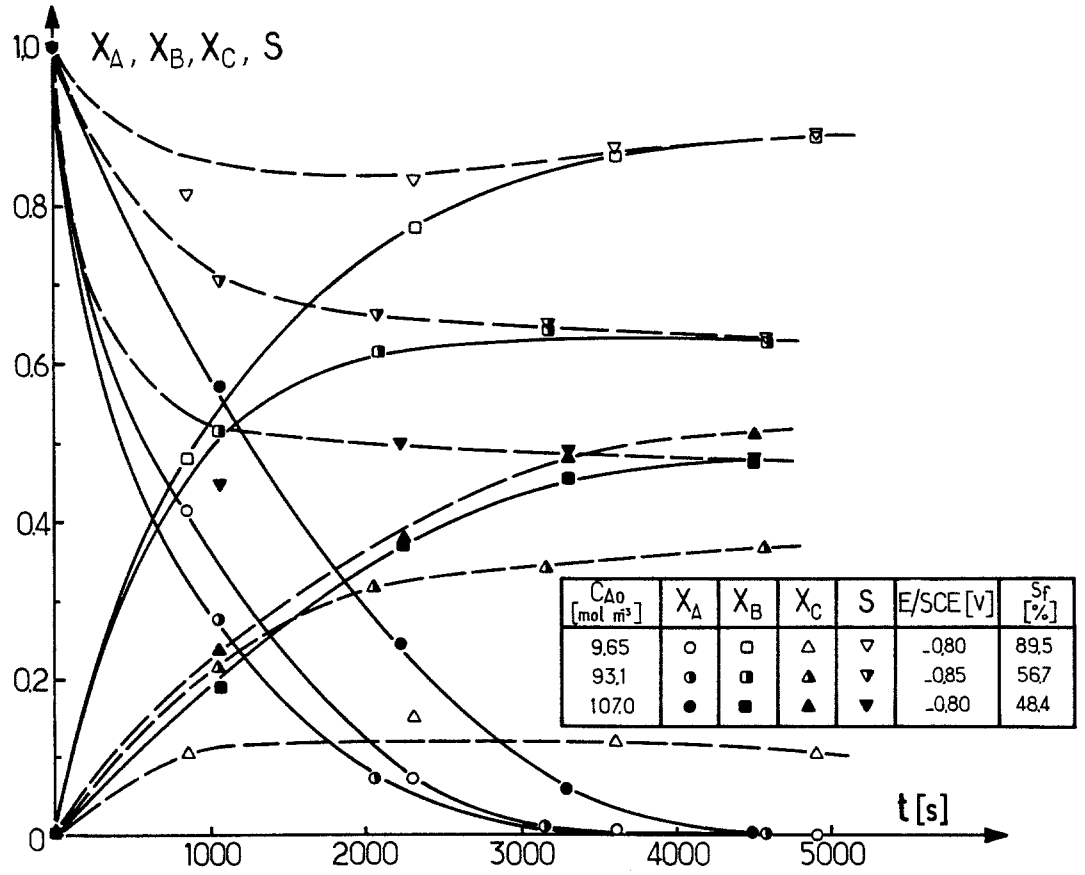

Fig. 8. Experimental time variations of the molar fractions X_A, X_B, X_C and selectivity, S, when $T = 298$ K; $N = 1000$ r.p.m; $a_e = 42.7\,m^{-1}$. Influence of the reactant initial concentration, C_{A0}.

prejudicial to a high selectivity. For $a_e = 42.7\,m^{-1}$ and $T = 298$ K, S drops from 89.53% to 48.36% when C_{A0} is increased from 9.55 to 106.9 mol m^{-3} (see Figs 8, 10). Again, two effects are to be considered if a higher concentration is used: an increase in the current intensity and therefore of the electrochemical reaction rate (favourable effect), but simultaneously an increase in the chemical reaction rate (undesired effect).

3.2.2.4. Experimental time variations of the operating current intensity. The variations of the operating current intensity, I, (measured experimentally under potentiostatic conditions) with the instantaneous concentrations, C_{AS}, are reported in Fig. 11 for the experimental conditions of Fig 9, characterized by low values of C_{A0} ($\simeq 10$ mol m^{-3}). The straight lines correspond to theoretical relations

$$I = I_L = v_e F k_d A_e C_{AS} \tag{6}$$

which should be valid if the following two conditions are verified at any time of the experiment:

(i) the maintained electrode potential defines pure diffusional conditions whatever the reactant concentration

(ii) the rate of the homogeneous chemical reaction is sufficiently low so that it has no effect on the concentration profiles of A and B inside the diffusion layer. The validity of this second condition will be discussed theoretically in Part II [7].

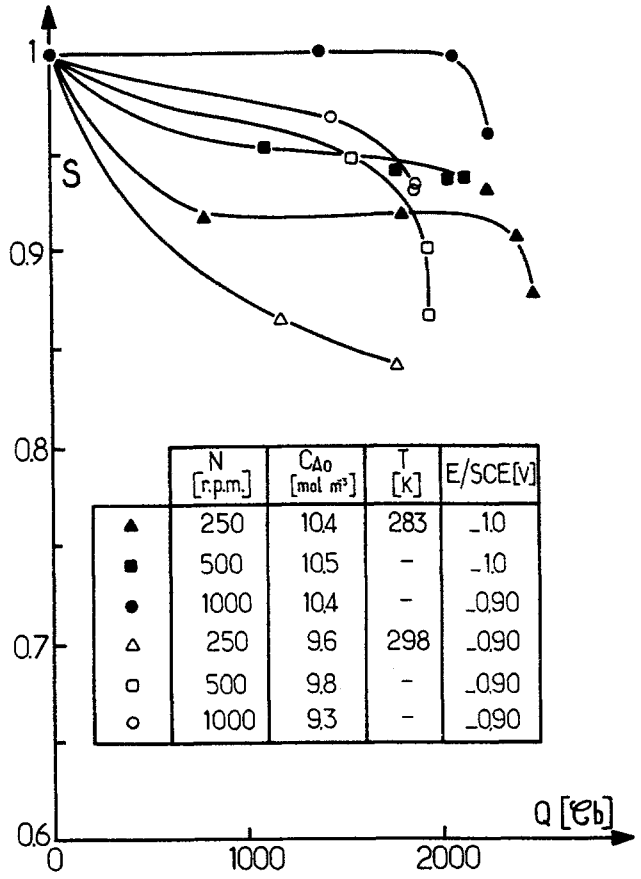

Fig. 9. Experimental variations of the selectivity, S, with the electrical charge, Q, when $a_e = 115.3\,m^{-1}$. Influence of the impeller rotation speed and the temperature.

At this point, it should be mentioned that this hypothesis is valid for the small initial concentration, C_{A0}, of Fig. 9, as it is confirmed by the comparison in Fig. 11 between the experimental values of I and the theoretical lines.

For higher concentrations (Fig. 12), the deviations between the experimental results and the theoretical lines become important (see, for example, the case where $C_{A0} = 106.9\,mol\,m^{-3}$). Two explanations may be proposed:

(i) the large inclination of the diffusion plateau for high values of C_{A0}, due probably to problems of current distribution

(ii) the effect of the chemical reaction inside the diffusion layer, leading to a modification of the profiles and the concentration gradient at the electrode. This point will be discussed in Part II of this work [7].

Finally, increase in the specific electrode area produces a higher current intensity and consequently a higher selectivity (see Fig. 10).

4. Conclusions

For a batch process, where unwanted homogeneous chemical reactions are coupled with a desired electrochemical reduction reaction, we have shown how different operating conditions (physicochemical, geometric and mixing structure) may yield very different values of the selectivity. In particular, the initial reactant concentration plays a significant role which demonstrates an important dilemma for the case considered in this study: the concentration should be as high as possible

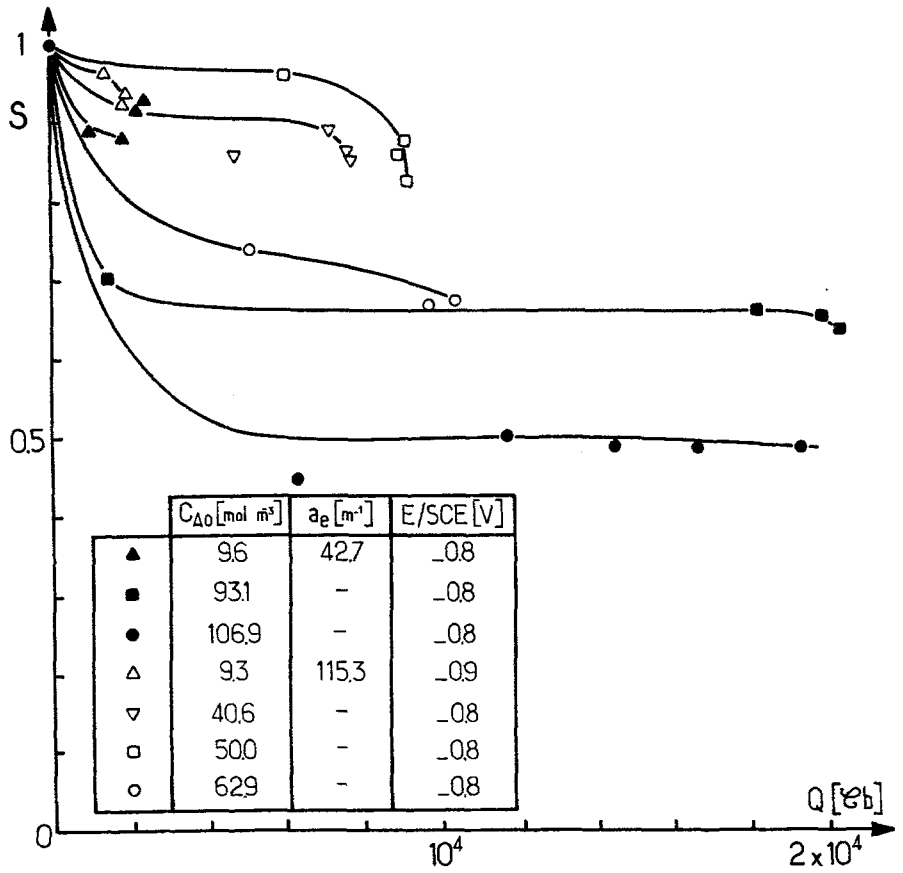

Fig. 10. Experimental variations of the selectivity, S, with the electrical charge, Q, when $T = 298\,\mathrm{K}$ and $N = 1000\,\mathrm{r.p.m.}$ Influence of the reactant initial concentration, C_{A0}, and specific electrode area, a_e.

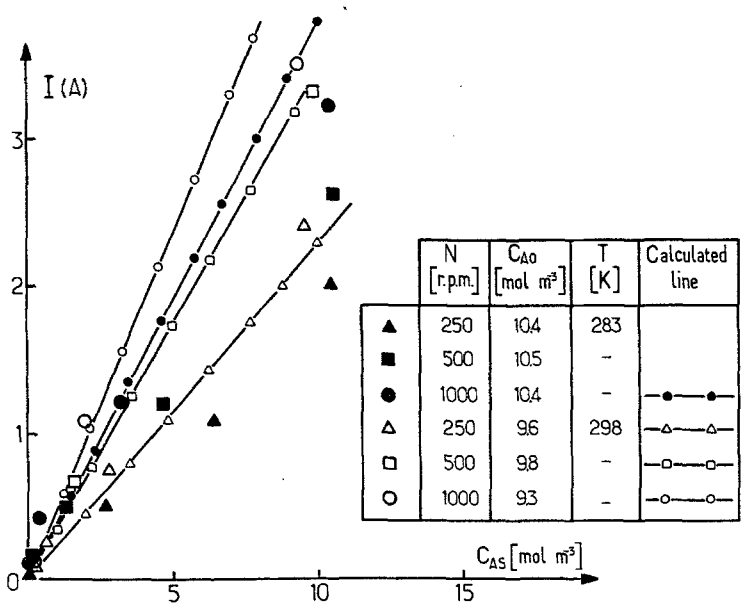

Fig. 11 Experimental variations of the current intensity, I, with the instantaneous reactant concentration, C_{AS}, when $A_e = 5.54 \times 10^{-2}\,\mathrm{m}^2$. Influence of the impeller rotation speed and the temperature.

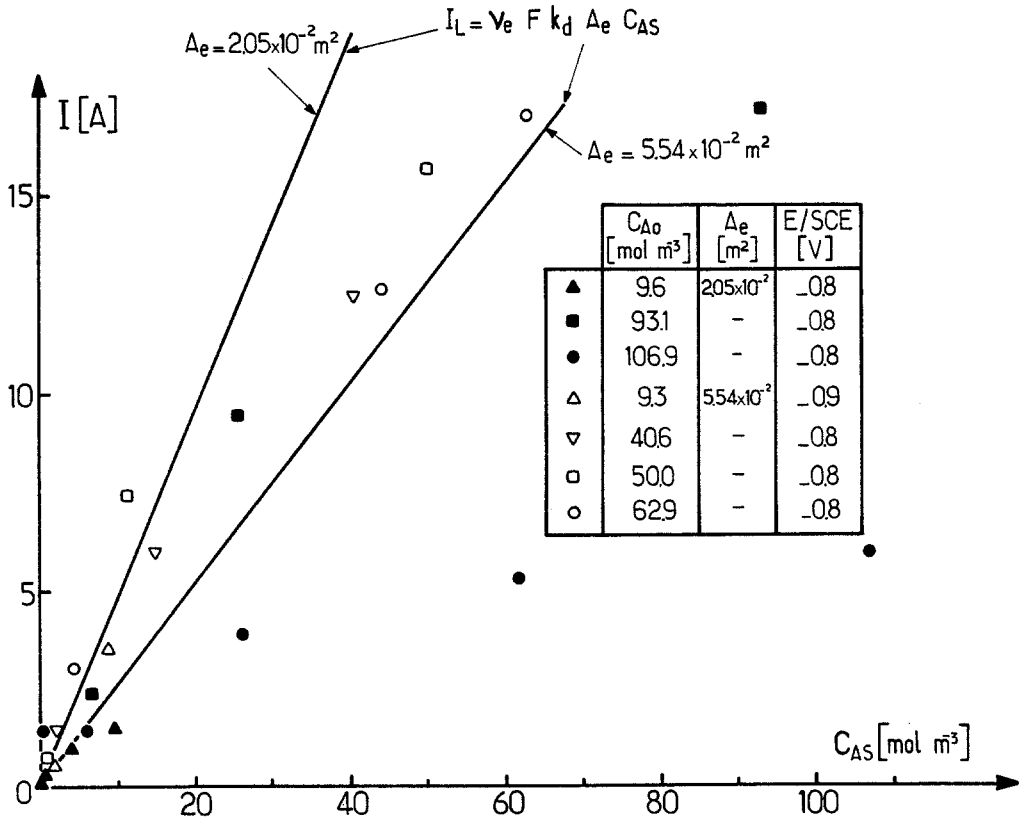

Fig. 12. Experimental variations of the current intensity, I, with C_{AS}, when $T = 298$ K and $N = 1000$ r.p.m. Influence of the reactant initial concentration, C_{A0}, and electrode area, A_e.

from the point of view of the capacity of production of the process and as small as possible from the point of view of the selectivity. Only empirical rules can be derived from an experimental approach. Some of these are evident, such as the necessity for using a high interfacial electrode area; others are more complicated, such as the effects of temperature and concentration. However, the design of a process to provide a given selectivity requires a better fundamental understanding of the coupling between chemical and electrochemical reactions, which is the subject of Part II of this work.

References

[1] N. R. Tomov and R. E. W. Jansson, *J. Chem. Tech. Biotechnol.* **30** (1980) 110.
[2] G. P. Sakellaropoulos and G. A. Francis, *ibid.* **30** (1980) 102.
[3] C. Amatore and J. M. Saveant, *J. Electroanal. Chem.* **123** (1981) 189.
[4] *Idem, ibid.* **123** (1981) 203.
[5] C. Amatore, F. M'Halla and J. M. Saveant, *ibid.* **123** (1981) 219.
[6] C. Amatore, J. Pinson and J. M. Seveant, *ibid.* **123** (1981) 231.
[7] L. Weise, G. Valentin and A. Storck, *J. Appl. Electrochem.* **16** (1986) 851.
[8] G. Jacob, C. Moinet and A. Tallec, *Electrochim. Acta* **27** (1982) 1417.
[9] G. Jacob, PhD Thesis, University of Rennes, France (1981).
[10] L. Weise, PhD Thesis, Institut National Polytechnique de Lorraine, Nancy, France (1986).